Two-dimensional electron-hole capture in a disordered hopping system

N. C. Greenham

Cavendish Laboratory, Madingley Road, Cambridge CB3 0HE, United Kingdom

P. A. Bobbert

Department of Applied Physics, Technische Universiteit Eindhoven, P.O. Box 513, NL-5600 MB Eindhoven, The Netherlands

We model the two-dimensional recombination of electrons and holes in a system where the mean free path is short compared with the thermal capture radius. This recombination mechanism is relevant to the operation of bilayer organic light-emitting diodes (LED's), where electrons and holes accumulate on either side of the internal heterojunction. The electron-hole recombination rate can be limited by the time taken for these charge carriers to drift and diffuse to positions where electrons and holes are directly opposite to each other on either side of the interface, at which point rapid formation of an emissive neutral state can occur. In this paper, we use analytical and numerical techniques to find the rate of this two-dimensional electron-hole capture process. Where one species of carrier is significantly less mobile than the other, we find that the recombination rate depends superlinearly on the density of the less mobile carrier. Numerical simulations allow the effects of disorder to be taken into account in a microscopic hopping model. Direct solution of the master equation for hopping provides more efficient solutions than Monte Carlo simulations. The rate constants extracted from our model are consistent with efficient emission from bilayer LED's without requiring independent hopping of electrons and holes over the internal barrier at the heterojunction.

I. INTRODUCTION

Transport and recombination processes in disordered hopping systems are of particular current interest since they determine the operation of light-emitting and photovoltaic devices based on organic and polymeric semiconductors. Where electrons and holes in these systems are free to move in three dimensions, their recombination can be successfully modeled using the Langevin approach. However, where the recombining particles are confined to move in a two-dimensional plane (for example on a surface or at the interface between two semiconductors), the physics becomes considerably more complicated. This is the problem which we address in this paper.

A particular situation where two-dimensional recombination may be important is in bilayer organic light-emitting diodes (LED's). Efficient electroluminescence can be achieved in small-molecule bilayer organic LED's, where electrons and holes are injected into electron-transporting and hole-transporting layers, respectively.[1] Similar structures can be formed in conjugated polymer LED's where the electron-transporting layer (ETL) can be spin coated on top of the hole-transporting layer.[2] In both types of device, the organic-organic heterojunction provides a barrier to the transport of both electrons and holes, leading to the accumulation of high densities of electrons and holes on either side of the interface. Typically, the carrier with the lowest barrier is injected over the barrier into the other layer, where it encounters a high density of opposite carriers with which it can recombine. Enhancement of efficiency results from preventing carriers escaping from the device without recombination, and from a redistribution of electric field within the device leading to improved balance of carrier injection.

Detailed information about carrier densities and electric fields in bilayer LED's can be obtained by numerical or analytical modeling of injection, drift, diffusion, and recombination processes.[3–5] Simple models have assumed that one carrier is first injected over the internal barrier, and then finds an opposite carrier with which to recombine in a Langevin-like process. Since there is a large backflow of injected carriers across the heterojunction, it is necessary to have a high density of charge carriers accumulated at the heterojunction in order to provide reasonable current densities in the device.[3,4] The accumulated charge carriers give an enhanced electric field at the heterojunction, which further assists the injection process. There is a concern that the high fields and carrier densities predicted by simple models might quench the excitons produced by recombination, leading to a reduction in overall device efficiency. A number of effects have been proposed which might enhance carrier injection at the heterojunction when one carrier arrives at a position exactly adjacent to an opposite carrier. If carrier injection can take place directly to form the bound exciton state (which is lower in energy than the single-particle electron and hole states by the exciton binding energy), then the barrier to charge transfer can be reduced, or even removed.[6] Even in the absence of any enhancement in the forward injection rate, rapid recombination with a carrier on the opposite side of the heterojunction will remove the possibility for backflow, thus increasing the net injection (and recombination) rate.[7] Furthermore, in some devices it is possible to form a neutral exciplex state directly at the heterojunction, without either carrier being injected over the barrier.[8] This exciplex may then itself decay radiatively, or may undergo energy transfer to an emissive excitonic state localized on one side of the heterojunction.

In each of these cases, the rate-limiting step in forming an emissive state is not the injection of carriers over the heterojunction, but rather the lateral motion of carriers in the plane

of the heterojunction to reach a position at which electron and hole are coincident on opposite sides of the heterojunction. The purpose of this paper is to determine the rate of this process by solving the two-dimensional drift-diffusion-recombination problem. We are thus able to investigate the consequences of this mechanism for the operation of bilayer organic LED's.

II. THE TWO-DIMENSIONAL RECOMBINATION PROBLEM

We consider the problem of electrons and holes arriving uniformly at a plane, in which they are then constrained to move. The carriers undergo diffusive motion, and also drift under their mutual coulomb attraction. Eventually, electrons and holes will meet, at which point rapid recombination is assumed to occur. We aim to model the overall recombination rate as a function of the mean electron and hole densities in the plane, n_A and p_A. In a heterojunction device, the electrons and holes will in fact be confined by the perpendicular electric field to a narrow region on opposite sides of the interface. For simplicity, however, we neglect the vertical separation between electrons and holes, and consider them to move within the same lateral plane. The full problem allowing both electrons and holes to move in their mutual Coulomb potential is very complex, and we therefore choose to consider one carrier (arbitrarily chosen to be the holes) to be fixed, and the other carrier (the electrons) to be mobile. Since the mobilities of electrons and holes on either side of an interface are seldom well matched, this approximation will frequently be justified in practice. We also neglect interactions between the electrons, which should have only a minor influence on the recombination rate under typical operating conditions where electron and hole densities are approximately equal. In practice, long-range Coulomb interactions will cause some correlation in arrival positions between electrons and holes. Nevertheless, there will typically be a strong electric field perpendicular to the interface which for most carriers will dominate over the long-range Coulomb attraction, justifying the assumption of uniform arrival flux mentioned above.

The problem of diffusion-limited two-dimensional recombination has previously been analyzed,[9] however here we wish also to include the drift of carriers due to their mutual Coulomb attraction. In organic semiconductors, carrier mean free paths are typically much shorter than the thermal Coulombic capture radius, so ballistic effects are negligible. The three-dimensional analog of this problem, known as Langevin recombination, has been extensively studied, and gives a recombination rate per unit volume of $(\mu_n + \mu_p)enp/\epsilon$, where n and p are the electron and hole densities, respectively, μ_n and μ_p are the electron and hole mobilities, ϵ is the permittivity of the medium, and e is the electronic charge. This result is obtained by integrating the drift flux of electrons through a spherical surface of radius r surrounding a hole. Since the electric field scales as r^{-2} and the surface area of the sphere scales as r^2, the value of r chosen is unimportant, leading to a simple solution with constant electron density, thus justifying the neglect of diffusion. In two dimensions, however, the problem is more complicated, since the electric field still scales as r^{-2}, but the integration now takes place over a circle of circumference $2\pi r$. To achieve a recombination current which is independent of r requires a density of electrons which varies with r. The presence of a carrier density gradient means that diffusion must be explicitly included in the problem. Solutions which consider a single recombination center give an electron density which diverges as $r \to \infty$, thus it is necessary to include a distribution of recombination centers in the problem.

III. APPROXIMATE ANALYTICAL SOLUTION

We begin by attempting to find an approximate analytical solution to the problem, using a continuum picture of drift and diffusion. The two-dimensional electron flux density in the plane, $\mathbf{J}(\mathbf{r})$, is related to the local surface density of electrons $n(\mathbf{r})$ by the sum of the drift and diffusion flux densities:

$$\mathbf{J}(\mathbf{r}) = -\mu n(\mathbf{r})\mathbf{E}(\mathbf{r}) - D\boldsymbol{\nabla}n(\mathbf{r}), \tag{1}$$

where μ is the surface mobility of the electrons, $\mathbf{E}$ the electric field, and D the diffusion constant. In this section, we will assume that D is related to μ by the Einstein relation $D = \mu kT/e$ where T is the absolute temperature. We will also assume that the mobility is independent of the electric field.

The electron density is maintained by a uniform influx f of electrons from the bulk onto the plane under consideration. For a surface density p_A of recombination sites, we consider each site to be surrounded by a "catchment area," with an average area of $1/p_A$, in which electrons arriving from the bulk will eventually be captured by that specific recombination site. At the boundaries between catchment areas we should have $\mathbf{J}(\mathbf{r}) = 0$. The central approximation in this section is the replacement of all catchment areas by identical disc-shaped regions with radius $r_c = 1/\sqrt{\pi p_A}$ in which we have a radial electric field $E(r) = e/4\pi\epsilon_0\epsilon_r r^2$ of just the hole at the center of each area. Throughout this paper we take $\epsilon_r = 4$. The flux density within each area should obey

$$\boldsymbol{\nabla} \cdot \mathbf{J}(\mathbf{r}) = f[1 - \pi r_c^2 \delta(\mathbf{r})], \tag{2}$$

where the uniform influx f is balanced by a removal term at the origin.

The radial flux density obeying this equation and satisfying the boundary condition $J(r_c) = 0$ is

$$J(r) = \frac{f}{2}\left(r - \frac{r_c^2}{r}\right). \tag{3}$$

Combination of Eq. (1) in its radial form and Eq. (3) leads to a first-order inhomogeneous differential equation for $n(\mathbf{r})$, which can readily be solved to give

$$n(r) = \frac{e}{\mu kT}\frac{f}{2}\left[\left(\frac{a^2}{2} - r_c^2\right)e^{a/r}\text{Ei}(-a/r) + \frac{1}{2}(ar - r^2)\right], \tag{4}$$

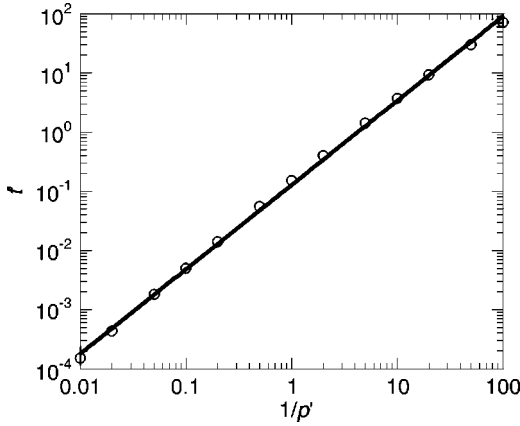where $a \equiv e^2/4\pi\epsilon_0\epsilon_r kT$ and $\text{Ei}(x)$ is the exponential integral function

FIG. 1. The function t' of Eq. (8), determining the recombination time of the two-dimensional recombination process, plotted vs the inverse reduced recombination site density $x_c^2 = 1/p'$ (circles), and a power-law fit to this function (line), $t' = 0.14(1/p')^{1.43}$.

$$\text{Ei}(x) = -\int_{-x}^{\infty} \frac{e^{-z}}{z} dz. \tag{5}$$

A quantity of specific interest is the recombination time $t = n_A/f$, the average time it takes for an electron to reach a recombination site after arrival at the surface [n_A is the surface average of $n(\mathbf{r})$]. Within our approximation, we have

$$t = \frac{2\pi \int_0^{r_c} dr\, r n(r)}{f\pi r_c^2}. \tag{6}$$

Introducing $x_c = r_c/a$ and performing the integral in this equation, we find the important result

$$t = \frac{e}{\mu kT} a^2 t'(x_c^2), \tag{7}$$

where $t'(x_c^2)$ is the function

$$t'(x_c^2) \equiv \left(x_c^2 - \frac{1}{2}\right) G_{23}^{31}\left(\frac{1}{x_c} \middle| \begin{matrix} 0,3 \\ 0,0,2 \end{matrix}\right) + \frac{1}{2} x_c\left(\frac{1}{3} - \frac{1}{4} x_c\right), \tag{8}$$

expressed in terms of a Meijer G function. The function t' is plotted versus the inverse reduced recombination site density $1/p' \equiv x_c^2 = 1/\pi p_A a^2$ in Fig. 1. The function can be described rather well by the power law $t' \approx 0.14(1/p')^{1.43}$. The surface recombination rate R is related to the recombination time by $R = n_A/t$. If t were linearly dependent on $1/p_A$, we could describe the recombination as a conventional bimolecular process with $R = \gamma_A n_A p_A$. However, due to the superlinear dependence of the recombination rate on the recombination site density p_A, the recombination process can only be described using second-order kinetics if the recombination rate is taken to depend on p_A, giving

$$R = \gamma_A(p_A) n_A p_A, \tag{9}$$

where $\gamma_A(p_A)$ is (weakly) dependent on p_A. In the following sections, we will investigate the problem in more detail within a numerical approach.

IV. MONTE CARLO SIMULATIONS

The analytical approach developed above provides a convenient universal solution, however it is limited in its treatment of the electric-field distribution, the need to define an effective "catchment area," and the assumption of a field-independent mobility. For a system where the transport is limited by energetic disorder, mobility measured on macroscopic length scales is found to vary with field as $\mu = \mu_0\exp(b\sqrt{E})$.[10] However, it is not clear that these mobilities can be applied directly in problems where the electric field varies significantly on microscopic length scales. To address these issues, we now attempt to simulate the two-dimensional recombination problem at a microscopic level using the Monte Carlo approach developed for disordered hopping systems by Bässler and co-workers.[11,12] This approach been successfully applied to describe transport processes in molecularly doped polymers and in conjugated polymers.[10]

For simplicity, we first consider a regular square lattice of recombination sites (holes) with separation L. We consider electrons arriving with a flux f within one unit cell of this lattice, and the aim is to determine the mean time for recombination of an arriving electron with a hole. The unit cell under consideration is divided into an array of $N \times N$ hopping sites of dimension d, where $d = 1$ nm. Electrons are then allowed to hop from their existing site (energy E_i) to a nearest-neighbor site (energy E_j) according to Miller-Abrahams hopping rates w_{ij}, where

$$w_{ij} = \begin{cases} \nu_0\exp\left(-\frac{(E_j - E_i)}{kT}\right) & \text{if } E_j > E_i \\ \nu_0 & \text{if } E_j < E_i. \end{cases} \tag{10}$$

Hopping energies are determined by first calculating the field at each hopping site due to a 100×100 lattice of holes centered on the unit cell under consideration. A random energetic disorder is then superimposed on the electrostatic energy at each site according to the probability distribution

$$p(E) = \frac{1}{\sigma\sqrt{2\pi}}\exp\left[-\frac{1}{2}\left(\frac{E - E_0}{\sigma}\right)^2\right]. \tag{11}$$

Cyclic boundary conditions are imposed so that electrons hopping out of one side of the unit cell reappear at the other side. Recombination is assumed to occur when the electron reaches a site with a positive charge at its corner. Electron densities are assumed to be small enough that state-filling effects within the distribution of site energies can be neglected.

In the Monte Carlo simulation, a random disorder configuration and a random arrival position were selected for each arriving electron. At each site occupied by the electron, the hopping rates k_u, k_d, k_l, and k_r for up, down, left, and right hops were calculated according to Eq. (10). The mean
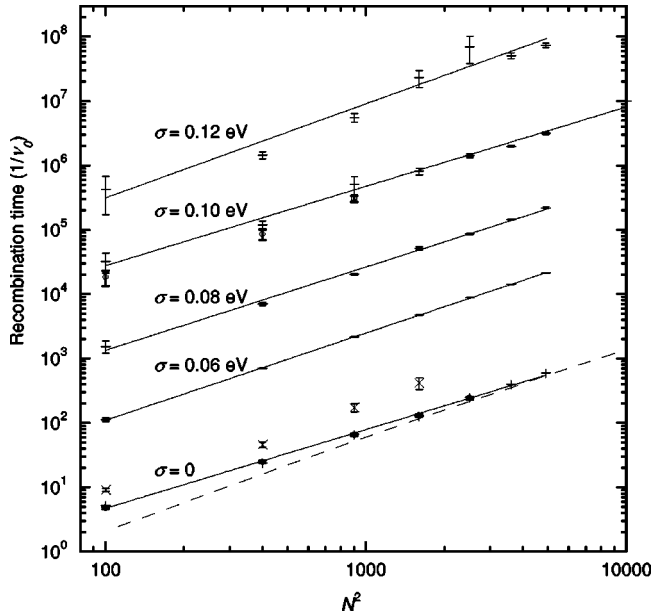
FIG. 2. Recombination time vs N^2 (inverse hole density) for various values of disorder (σ) as labeled. For all simulations the temperature T was 300 K, and the spacing between lattice sites was 1 nm. $\bigcirc$'s represent Monte Carlo results and $+$'s represent master equation results. Solid lines represent fits to the master equation results, and the dashed line represents the approximate analytical result of Sec. III using the same parameters. Results shown are for regular lattices of recombination centers, except $\times$'s which represent master equation results for a random lattice of recombination centers with $\sigma=0$.

hopping time $\tau=(k_u+k_d+k_l+k_r)^{-1}$ was calculated, and an actual hopping time t_h was selected randomly from a distribution $p(t_h)=(1/\tau)\exp(-t_h/\tau)$. Total recombination times were then recorded for m arriving electrons, and used to calculate a mean recombination time t. Figure 2 shows the recombination time as a function of hole density for $\sigma=0$ and $\sigma=0.1$ eV (a typical value for disorder in organic systems). For $\sigma=0$, $m=500$ was sufficient to obtain reasonable statistics. For $\sigma=0.1$ eV, the statistics were more problematic, since the mean recombination time was dominated by the tail of the distribution of recombination times where the recombination was particularly slow (since the electron was trapped at a deep minimum in the disorder). Larger values of m (between 2000 and 5000) were therefore used, and there is considerable uncertainty in the magnitude of the error bars shown.

V. MASTER EQUATION SIMULATIONS

Monte Carlo techniques proved unfeasibly slow for large N in the presence of disorder, so to obtain a larger dataset an alternative approach was used, based on direct solution of the master equation.[13] The hopping sites within the unit cell are labeled $i=1,\ldots,N^2$, and the steady-state population of each site p_i satisfies

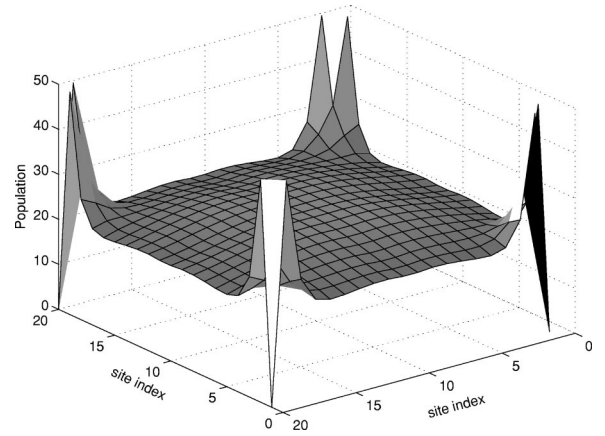$$\frac{dp_i}{dt}=f_i+\sum_j (w_{ji}p_j-w_{ij}p_i)=0, \qquad (12)$$

FIG. 3. Carrier population per site as a function of position for $N=20$, $\sigma=0$, determined by solving the master equation with $\nu_0=1$ Hz.

where f_i is the flux arriving at the ith site. This equation can be recast in matrix form

$$\sum_j M_{ij}p_j=-f_i, \qquad (13)$$

where

$$M_{ii}=-\sum_j w_{ij} \qquad (14)$$

and

$$M_{ji}=w_{ij}, \quad j\neq i. \qquad (15)$$

M is a sparse matrix, with entries on nine diagonals to account for up, down, left, and right jumps, including jumps where the cyclic boundary conditions are invoked. Equation (13) was solved using standard matrix routines within MATLAB, to give the carrier population as a function of position for various value of N. The mean recombination time was then calculated as $\Sigma_i p_i/\Sigma_i f_i$. Initially we assumed that carriers arrive equally at each site such that $f_i=1$ for all i. The problem is linear in **f** so the value of f_i is unimportant in determining t.

Figure 3 shows the carrier density in one unit cell for $N=20$ and $\sigma=0$. Away from the region immediately surrounding the recombination center, the carrier density increases with distance from the recombination center. The buildup of carrier density close to the recombination center is a consequence of the high field, which for Miller-Abrahams hopping rates in the absence of disorder causes a decrease in mobility with respect to the low-field value. For a field-independent mobility [Eq. (4)], the carrier density would scale linearly with r for small r. However, since the number of carriers in the region of high field is a small fraction of the total number of carriers, this effect does not significantly alter the calculated recombination time for large N. For larger values of σ, such as $\sigma=0.1$ eV, for example, the carrier density is strongly dominated by the energetic disorder, with variations of more than four orders of magnitude between different sites, and the recombination time is sensitive

TABLE I. Exponent s determined from an unweighted least-squares fit of the data in Fig. 2 to the equation $t \propto (N^2)^s$.

σ (eV)	s
0	1.22 ± 0.02
0.6	1.35 ± 0.01
0.8	1.29 ± 0.03
1.0	1.23 ± 0.05
1.2	1.46 ± 0.14

to the exact random configuration of disorder. To obtain reliable mean recombination times it is therefore necessary to average over a large number of disorder configurations. In the following work Eq. (13) was solved 1000 times for different random disorder configurations to obtain a mean recombination time. Figure 2 shows the recombination time as a function of inverse hole density for various values of σ. As expected, the values calculated using the master equation agree to within the statistical error with the results of the Monte Carlo simulations discussed earlier. The recombination time increases markedly with increased disorder, due to the lower mobility. Relative uncertainties in the recombination time also increase with disorder, due to the larger variation between individual random disorder configurations. The recombination time scales superlinearly with the inverse carrier density, with $t \propto (N^2)^s$. Best-fit values of s are shown in Table I. The values of s are typically slightly smaller than the value of 1.43 predicted by the analytical model. This is partly due to the different electrical field patterns taken in the two models, and, for $\sigma = 0$, partly because the reduced mobility near the recombination centers becomes less important for large N. For $\sigma = 0$, at large N ($N \gtrsim 40$) the numerical results are larger than the analytical result by a geometrical factor of only about 1.1.

In the case of $\sigma = 0$, ν_0 is related to the low-field mobility by

$$\mu = \frac{\nu_0 e d^2}{kT}. \tag{16}$$

Using Eq. (16), we obtain

$$\gamma_A = \frac{kT}{p_A t \nu_0 e d^2} \mu. \tag{17}$$

For $N = 20$ (corresponding to $p_A = 2.5 \times 10^{15}$ m^{-2}), this becomes

$$\gamma_A = (0.43 \text{ V}) \mu. \tag{18}$$

From the analytical continuum solution [Eq. (4)], one would expect γ to scale linearly with μ, and hence Eq. (18) should apply generally for given values of N and temperature. If this is true in the microscopic model, then disorder should have the same effect on γ_A as on mobility. Figure 4 shows the relative variation of γ with σ for $N = 20$. The effect of disorder on mobility for three-dimensional transport has been studied extensively by Bässler and co-workers, who find that the zero-field mobility scales as
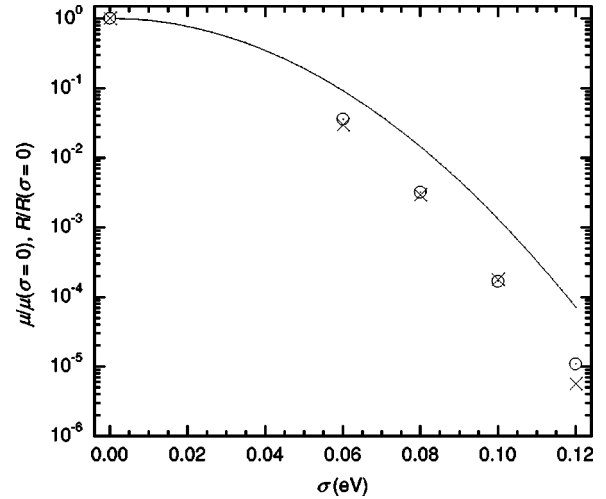

FIG. 4. Relative recombination rate as a function of disorder, σ, for $N = 20$ ($\odot$). Variation of relative mobility with σ is also shown, for 3D mobility according to Eq. (19) (line) and for the 2D simulation described in the text ($\times$).

$$\mu = \mu_0 \exp\left[-\left(\frac{2\sigma}{3kT} \right)^2 \right] \tag{19}$$

in the absence of positional disorder.[11,12] As can be seen from Fig. 4, the recombination rate decreases more quickly with increasing disorder than the three-dimensional (3D) mobility from Eq. (19). However, in the recombination problem considered here the carriers are confined to move only in two dimensions, and are therefore unable to move in the third dimension to avoid particularly high-energy sites. Hence one would expect the two-dimensional mobility to be more sensitive to disorder than the three-dimensional mobility. Quantitative simulations of 2D mobility were therefore performed using the same master equation approach described above. In this case, though, a constant small electric field of 10^4 V m^{-1} was applied over a 40 nm $\times$ 40 nm square. Carriers were supplied with a constant flux along one edge of the square, and removed along the other edge. Under these low-field conditions, the current was dominated by diffusion, and diffusion coefficients were extracted from the mean carrier density gradient, averaging over the square and over 100 000 different random disorder configurations for each value of σ. As can be seen from Fig. 4, the diffusion coefficient (and hence the mobility) varies with disorder in a very similar fashion to the recombination rate. This confirms that the recombination rate does indeed scale with the relevant 2D mobility.

In the results above, it was assumed that the carriers arrive uniformly at the interface. This assumption ignores the relaxation within the Gaussian density of states which may occur as carriers are injected into and transported through the device. To test the opposite limit of full relaxation, the incoming flux was adjusted to have the form

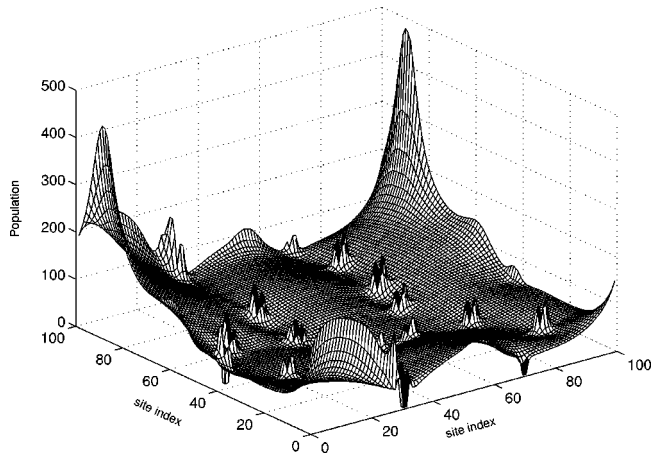$$f_i = f_0 \exp\left(\frac{-E_i}{kT} \right). \tag{20}$$

FIG. 5. Carrier population per site as a function of position for a random lattice of recombination centers with an average density equal to that in Fig. 3 ($N=20$).

With $N=20$ and $\sigma=0.1$ eV, this was found to give a reduction in the recombination rate by a factor of ≈ 4.

In a further refinement to the model, the effect of allowing a random distribution of recombination sites was examined. The problem was solved on a 100×100 grid, with cyclic boundary conditions. A random hole distribution with a specified mean density was then generated. The electric field was calculated including not only the holes within the 100×100 grid, but also a random distribution of holes in a 600 nm$\times$600 nm area centered on the grid. A sample steady-state carrier distribution with $\sigma=0$ is shown in Fig. 5. Recombination times for $\sigma=0$ are shown in Fig. 2, for $N=10$–40, averaging over 20 random distributions of holes. With the random distribution of recombination sites, the recombination rate is reduced by roughly a factor 2 compared with a regular lattice.

VI. DEVICE MODELING

In this section, we will apply the results obtained above to investigate charge densities and electric fields in bilayer

LED's. Devices were modeled by numerically solving the drift-diffusion-recombination equations for electrons and holes, allowing for the effect of internal charges on the electric field within the device. Figure 6(a) shows the results where electrons and holes are required to jump over a barrier at the heterojunction, followed by Langevin-like recombination with opposite charges. Figure 6(b) shows the case where no carriers are allowed to jump over the barrier, but two-dimensional recombination is taken to be the rate-limiting step in exciton (or exciplex) formation at the interface. In both cases, ohmic injection was assumed at the electrodes, and, for simplicity, constant mobilities of 10^{-5} cm^2 V^{-1} s^{-1} were used for both carriers. For case (a), barriers of 0.6 eV and 0.9 eV were used for hole and electron injection, respectively, roughly the values found in bilayer devices based on poly(p-phenylenevinylene) and its cyanosubstituted derivative CN-PPV.[2] The smaller barrier for hole injection leads to recombination overwhelmingly in the ETL. The model for carrier injection was similar to that reported by Staudigel et al.,[4] which considers thermal injection and backflow at the heterojunction with a Gaussian density of states of width 0.1 eV, but neglects carrier relaxation effects. For the numerical simulation, the device was divided into slices of thickness 1 nm. Although the details of this model are open to question, the main result is clear: there is a large buildup of electrons and holes at the interface, leading to a significantly enhanced electric field. Both effects promote charge injection over the barrier.

In case (b), carriers within 1 nm of the interface are allowed to recombine by two-dimensional motion according to Eq. (18). We use a lateral mobility of 10^{-5} cm^2 V^{-1} s^{-1}, the same value as the perpendicular mobility. To account for the motion of both carriers, we use an "effective mobility" of twice the mobility of the individual carriers. A problem then arises in the functional dependence of the recombination rate on the electron and hole densities when both carriers have equal mobilities, since Eq. (9) is not symmetric in electron and hole density. To avoid this problem, we use Eq. (9) with a constant γ determined by Eq. (18), which is valid for carrier surface densities of the order of 2.5×10^{15} m^{-2} (corre-
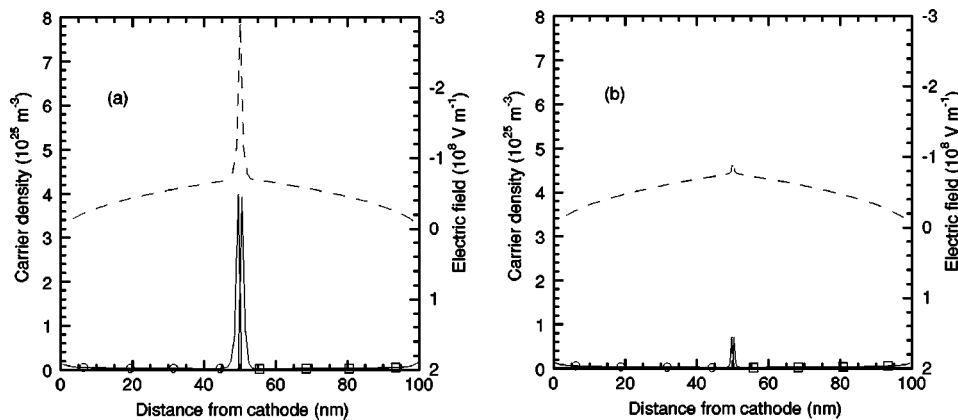

FIG. 6. Electron density ($\bigcirc$), hole density ($\square$), and electric field (dashed line) as a function of position in a device with an internal voltage of 5 V. (a) represents a device where recombination occurs after hopping over the interfacial barrier (0.6 eV for holes and 0.9 eV for electrons). (b) represents a device where recombination is limited by two-dimensional recombination. Other details are given in the text. The current densities predicted were 1950 A m^{-2} and 2187 A m^{-2} for (a) and (b), respectively.

sponding to volume densities around 2.5×10^{24} m^{-3} in the first 1 nm of polymer). The results shown in Fig. 6 confirm that the interfacial charge densities are indeed in this range. These densities are small compared with the site density, justifying our neglect of state-filling effects in the microscopic simulation of recombination rates. In conjugated polymer devices, the in-plane mobility (measured in field-effect transistors) is in fact found to be significantly higher than the perpendicular mobility (extracted from modeling space-charge-limited currents), due at least in part to the preferential alignment of chains in the plane of the device. Hence, irrespective of the uncertainties discussed above, the simulation is likely to underestimate the true recombination rate in real devices, and the calculated interfacial carrier densities represent an upper limit.

The simulations therefore show that efficient recombination can occur in the case where formation of neutral excited states is limited by lateral drift and diffusion of charge carriers at the interface. This process leads to some buildup of charge density at the interface, but this can be much less than is necessary when charges have to be injected over typical barriers before recombination. We note that in case (b) the interfacial charge densities will scale with light output L as L^r where $r < 0.5$, which allows high intensities to be achieved with reasonable charge densities. The slight increase of electric field at the interface is a consequence of the buildup of charge density, and does not itself assist the recombination. This contrasts with case (a) where the increased electric field plays a major role in promoting injection of carriers over the barrier. We note that mechanism (b) can work equally well in a polymer blend device where interfaces are not necessarily perpendicular to the external electric field. The calculated current densities are similar in both (a) and (b), which indicates that the additional voltage drop produced by the carrier buildup at the interface is small compared with the applied voltage, and hence both devices will show similar current-voltage characteristics limited by the bulk mobility. However, the high fields and charge densities present at the interface in case (a) could be damaging to the efficiency of the device, since they may provide additional nonradiative decay channels for excitons which will be produced close to the interface.

VII. CONCLUSIONS

We have modeled the process of electron-hole capture by drift and diffusion within a plane. There is good agreement between analytical approximations and microscopic simulations. The effect of energetic disorder has been examined, and has been found to have a similar effect on two-dimensional mobility as on the recombination rate. The process can therefore be conveniently parametrized in terms of a two-dimensional mobility. Direct solution of the microscopic hopping problem using the master equation approach provides more rapid solutions than Monte Carlo simulations, and has allowed systems with a random distribution of recombination sites to be studied. Rate constants derived from these simulations have been used to set boundary conditions in numerical models of charge and field distributions in bilayer organic devices, which has shown that only modest buildup of charge densities is required at the interface when recombination is limited by two-dimensional drift and diffusion of carriers to adjacent sites where rapid formation of the emissive state can occur. These results help to explain the efficient operation of polyfluorene blend LED's, where emission has recently been shown to occur via an exciplex state which can form without hopping of either carrier over the heterojunction barriers.[8] Our model for the rate of two-dimensional recombination may also find application in other areas, for example in the study of chemical reactions between charged species on a surface.

ACKNOWLEDGMENTS

[1] C.W. Tang and S.A. VanSlyke, Appl. Phys. Lett. **51**, 913 (1987).

[2] N.C. Greenham, S.C. Moratti, D.D.C. Bradley, R.H. Friend, and A.B. Holmes, Nature (London) **365**, 628 (1993).

[3] B.K. Crone, P.S. Davids, I.H. Campbell, and D.L. Smith, J. Appl. Phys. **87**, 1974 (2000).

[4] J. Staudigel, M. Stössel, F. Steuber, and J. Immerer, J. Appl. Phys. **86**, 3895 (1999).

[5] V.R. Nikitenko, O.V. Salata, and H. Bässler, J. Appl. Phys. **92**, 2359 (2002).

[6] S. Cina, N. Baynes, E. Moons, R.H. Friend, J.H. Burroughes, C.R. Towns, C. Heeks, R. O'Dell, S. O'Conner, and N. Anthanassopoulou, Proc. SPIE **4279**, 221 (2001).

[7] V.I. Arkhipov, E.V. Emelianova, and H. Bassler, J. Appl. Phys. **90**, 2352 (2001).

[8] A.C. Morteani, A.S. Dhoot, J.S. Kim, C. Silva, N.C. Greenham, R.H. Friend, C. Murphy, E. Moons, S. Ciná, and J.H. Burroughes, Adv. Mater. **15**, 1708 (2003).

[9] D.L. Freeman and J.D. Doll, J. Chem. Phys. **78**, 6002 (1983).

[10] M. Van der Auweraer, F.C. De Schryver, P.M. Borsenberger, and H. Bässler, Adv. Mater. **6**, 199 (1994).

[11] G. Schönherr, H. Bässler, and M. Silver, Philos. Mag. B **44**, 47 (1981).

[12] H. Bässler, Phys. Status Solidi B **175**, 15 (1993).

[13] Z.G. Yu, D.L. Smith, A. Saxena, R.L. Martin, and A.R. Bishop, Phys. Rev. B **63**, 085202 (2001).